

DEPENDENCE OF TRANSFORMER CORE LOSS

ON CORNER JOINT CONSTRUCTION

A Thesis

Presented to

The Department of Electrical Engineering

The Faculty of Engineering

The University of Manitoba

In Partial Fulfillment

of the requirements for the degree

Master of Science in Electrical Engineering

by

D. H. Deneschuk

March, 1974

DEPENDENCE OF TRANSFORMER CORE LOSS
ON CORNER JOINT CONSTRUCTION

by

D.H. Deneschuk

A dissertation submitted to the Faculty of Graduate Studies of
the University of Manitoba in partial fulfillment of the requirements
of the degree of

Master of Science

© 1974

Permission has been granted to the LIBRARY OF THE UNIVERSITY OF MANITOBA to lend or sell copies of this dissertation, to the NATIONAL LIBRARY OF CANADA to microfilm this dissertation and to lend or sell copies of the film, and UNIVERSITY MICROFILMS to publish an abstract of this dissertation.

The author reserves other publication rights, and neither the dissertation nor extensive extracts from it may be printed or otherwise reproduced without the author's written permission.

ABSTRACT

The design of corner joints in a power transformer core can have a pronounced effect on the total core loss, and hence on the efficiency of the whole transformer. An experimental model was built in which the method of stacking the laminations and overlap lengths of the mitered joint corners were varied to study the effect on the core loss. This effect was detected by a change in area of the hysteresis curve displayed on an oscilloscope.

ACKNOWLEDGEMENT

The author wishes to express his appreciation to Professor G.W. Swift of the Electrical Engineering Department, University of Manitoba for his most patient guidance and assistance throughout this project, and to Mrs. J. Deneschuk for her kind assistance in core assembly. Thanks are expressed to Federal Pioneer Electric for the supply of core steel and interest in this work.

LIST OF ILLUSTRATIONS

FIGURE	PAGE
2:1 Experimental Transformer Core	2
2:2 Typical Hysteresis Curve	3
2:3 Model Transformer Core	4
2:4 Representative Hysteresis Curve	5
2:5 Determination of Eddy Current Loss In A Lamination	6
3:1 Integration Circuit Used to Obtain $\int \text{edt}$	8
3:2 Hysteresis Trace on Sample Grid	11
4:1 45° Mitered Overlap Joint of Overlap Length L	14
4:2 45° Mitered Overlap Joint of Overlap L and Airgap g	14
4:3 Alternate Lapping Core Configuration	14
4:4 Constructed Step-Lap Configuration	15
4:5 Photograph and Schematic of Experimental Set Up	16
4:6 Photograph of Excitation Winding on Transformer Core .	18
4:7 Rectified Average Digital Readout Voltmeter	20
4:8 Typical Hysteresis Curve	20
5:1 Comparison of Measuring Techniques	23
5:2 Experimental Results of Alternate Lapping	25

LIST OF TABLES

	<u>PAGE</u>
Table of Construction Variables.....	13
Table of Power Loss Values at 1.36 Tesla.....	22
Table of Comparison of Experimental Variables.....	24
Table of Variation of Core Loss with Air Gap at an Overlap Distance $L = 2$ cm.....	27
Table of Power Transformer Specifications.....	29
Table of Volt-Ampere Input Data.....	33

TABLE OF CONTENTS

	PAGE
ABSTRACT.....	ii
ACKNOWLEDGEMENT.....	iii
LIST OF FIGURES.....	iv
LIST OF TABLES.....	v
CHAPTER	
I. INTRODUCTION.....	1
1:1 Core Loss in Mitered Joint Cores.....	1
II. THEORETICAL ANALYSIS.....	2
2:1 Transformer Action.....	2
2:2 Magnetic Circuits and AC Operation.....	3
2:3 Eddy Current Losses.....	6
III. DESIGN OF EXPERIMENTAL SET-UP.....	8
3:1 Integrator Circuit	8
3:2 Dimensions of Experimental Model.....	9
3:3 Flux Density Measurement.....	9
3:4 Power Loss Measurement.....	9
IV. EXPERIMENTAL INVESTIGATIONS.....	12
4:1 Core Construction Methods.....	12
4:2 Apparatus & Test Set-Up	12
4:3 Power Loss Measurement.....	17

CHAPTER		PAGE
V.	EXPERIMENTAL RESULTS & ANALYSIS.....	21
	5:1 General.....	21
	5:2 Single Lamination Results.....	24
	5:3 Double Lamination Results.....	27
	5:4 Air Gap Considerations.....	27
	5:5 Step-Lap Considerations.....	28
	5:6 Application to a Practical Case.....	28
VI.	CONCLUSION.....	31
	BIBLIOGRAPHY.....	32
	APPENDIX A.	33
	APPENDIX B.....	34

CHAPTER I

Introduction

1:1 Core Loss In Mitered Joint Cores

The efficiency of large power transformer cores depends upon to a large extent the core and winding losses. In many instances core loss becomes the major design factor. The core loss is made up of two main components, viz ., that due to hysteresis and that due to eddy currents. Hysteresis can be thought of as an energy loss when a magnetic material is in a cyclic state of magnetization due to some internal resistance which prevents the magnetization process from becoming completely reversible. Eddy current loss is the product of the resistance (to the path of eddy current flow) times the square of the eddy current magnitude. Both losses appear as heat in the core. The hysteresis and eddy current loss per cycle may be represented by the area of the "dynamic" hysteresis curve.

The efficiency of the transformer core depends to some extent on the type of corner joint used, since it is in this region where the flux deviates from the rolling direction of the steel; hence increased power losses. Previous experimental research has been minimal, and for this reason it was felt that as a first procedure, duplication of the results (for single lamination staggering of Jones)⁽¹⁾ would aid in confirming the measuring technique.

In this thesis, methods of stacking the laminations, air gap in the corner joint, and overlap length in the core have been varied and their effect on the power loss has been determined.

CHAPTER II

Theoretical Analysis

2.1 Transformer Action

Consider the theoretical one piece transformer core of cross-sectional area A shown below in Fig 2.1.

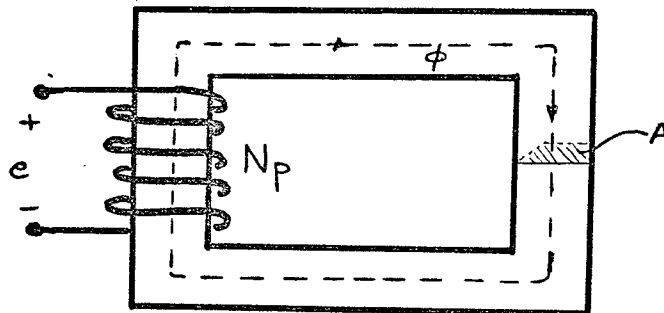


Fig. 2.1 THEORETICAL TRANSFORMER CORE

The instantaneous emf induced into the primary winding is expressed as

$$e = N_p \frac{d\phi}{dt} \quad \text{volts} \quad (2.1)$$

Assuming the flux in the core to be sinusoidal,

$$\phi = \phi_m \sin \omega t \quad \text{Wb.} \quad (2.2)$$

$$\text{it follows that } \phi = B_m A \sin \omega t \quad \text{Wb.} \quad (2.3)$$

where B_m is the maximum value of flux density in webers/m² and A is the cross sectional area of the core. Equation 2.1 may be rewritten as

$$e = \omega B_m A N_p \cos \omega t \quad \text{volts} \quad (2.4)$$

Equation 2.4 may be also expressed in terms of RMS quantities

$$E_{rms} = 4.44 f N_p B_m A \quad \text{volts} \quad (2.5)$$

Equation 2.5 is often referred to as the "transformer equation." In transformer design it is often useful to express the above equation in volts

per turn.

$$\frac{E_{rms}}{N_p} = 4.44 f B_m A \quad \text{volts/turn} \quad (2.6)$$

2.2 Magnetic Circuits and A.C. Operation

The basic law governing the relationship between electric current and magnetic field is Ampere's Law

$$\int \mathbf{J} \cdot d\mathbf{a} = \oint \mathbf{H} \cdot d\mathbf{l} \quad (2.7)$$

which merely becomes

$$Ni = Hl \quad (2.8)$$

where Ni is the total ampere turns.

The magnetic field intensity H produces a magnetic flux density B wherever it exists, of value

$$B = \mu H \quad (2.9)$$

The term μ is the permeability and is a property of the material.

The manner in which B varies with H may be seen in the typical magnetization (or simply BH) curve shown below in Fig. 2.2

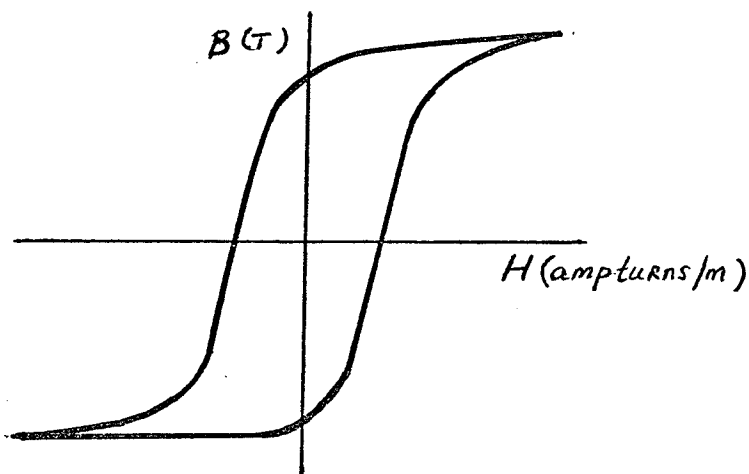


Fig. 2.2 TYPICAL HYSTERESIS CURVE

It can be shown that the area of the above curve is the hysteresis loss per cycle.

Consider Fig 2.3 shown below .

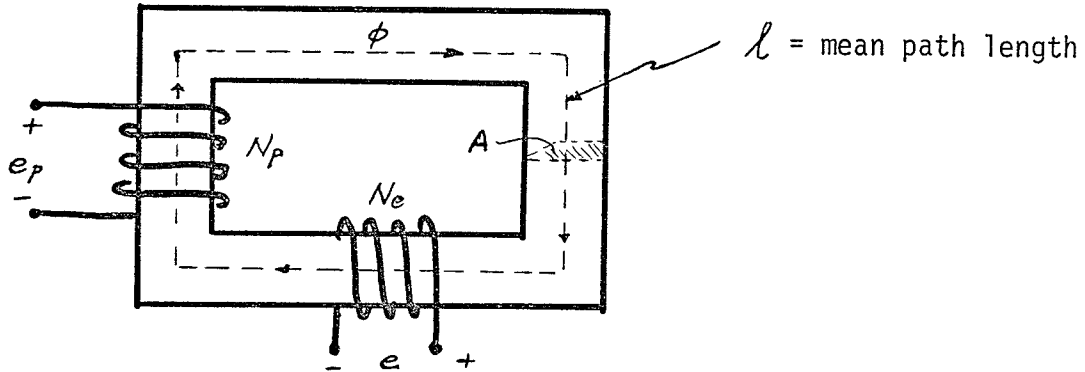


Fig. 2.3 MODEL TRANSFORMER CORE

The units of area are $B \times H$ which are

$$\frac{\text{webers}}{\text{m}^2} \times \frac{\text{amp-turns}}{\text{m}} = \frac{\text{joules}}{\text{m}^3 \text{ cycle}}$$

which is the energy loss in joules per unit element of volume, per cycle.

Mathematically, the energy loss W_0 is given by

$$W_0 = \oint B \, dH \quad \frac{\text{joules}}{\text{m}^3 \text{ cycle}} \quad (2.10)$$

where the integration is taken over one cycle.

The flux density B may be obtained by combining equations 2.1 & 2.3 to obtain

$$B = \frac{1}{N_e A} \int e \, dt \quad \frac{\text{Wb}}{\text{m}^2} \quad (2.11)$$

The magnetic field intensity H may be determined from equation 2.8,

$$\text{with } N = N_p, \quad H = \frac{N_p i}{l} \quad \frac{\text{A}}{\text{m}} \quad (2.12) \quad (2.12)$$

Combining equations 2.11 and 2.12

$$B \times H = \frac{N_p i}{N_e A_l} \int e dt \quad (\text{watts}) \quad \text{joules/m}^3$$

The total loss for the transformer core at 60hz would be

$$P_o = 60 \frac{N_p}{N_e} A_o \quad \text{watts} \quad (2.13)$$

where $A_o = i \times \int e dt$ as shown in Fig. 2.4 (2.13a)

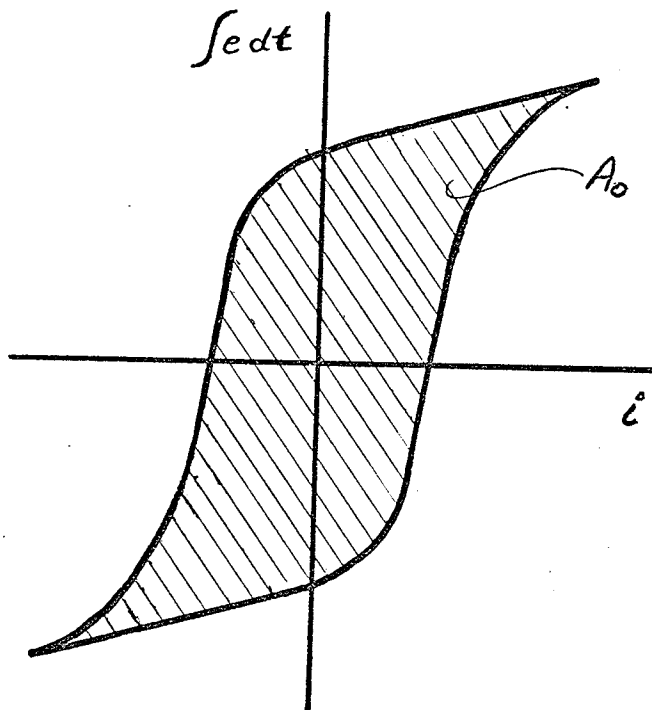


Fig. 2.4 Representative Hysteresis Curve

2.3 Eddy Current Losses

Steinmetz (2) has derived an approximate expression for the eddy current losses within a laminated magnetic material. Fig. 2.5 shows the cross sectional area of a lamination of thickness c , width y , and length z .

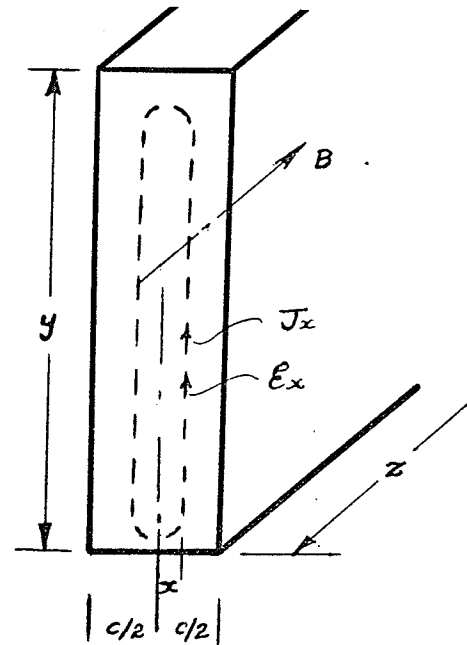


Fig. 2.5 The determination of eddy current loss in a lamination.

The sides of magnetic path are at distance x from the centre line of the lamination. This path encloses a flux

$$\phi = 2xyB \quad \text{webers}$$

Assuming $y \gg x$, application to Faraday's law yields

$$E_x = 2y \frac{d\phi_x}{dt}$$

Combining the above two equations gives

$$E_x = x \frac{dB}{dt}$$

The current density is therefore

$$J_x = \frac{x}{\rho} \frac{dB}{dt}$$

where ρ is the resistivity of the material. The total power loss in the lamination is found by integrating the loss density over the volume V . Averaged over the volume cyz of the lamination, the instantaneous power loss per unit volume is

$$P = \frac{c^2}{12\rho} \left(\frac{dB}{dt} \right)^2$$

If the flux density is alternating at angular frequency ω as given by

$$B = B_m \sin \omega t$$

the average eddy current loss per unit volume is

$$P = \frac{(c \omega B_m)^2}{24\rho} \quad (2.14)$$

The predictions of equation 2.14 that eddy current losses vary as the square of the lamination thickness, the square of the turns ratio and the square of the maximum value of flux density -- are often found to be inaccurate when compared to measured values of loss.

In any event, the eddy current losses produce a widening of the hysteresis loop of Fig. 2.4, so that the area of that loop is actually the total of the hysteresis and eddy current losses; i.e. the loop area is proportional to the total core loss.

CHAPTER III

Design of Experimental Set Up

3.1 Integrator Circuit

Examination of equation 2.13a reveals that the integral (with respect to time) of the search coil voltage e is necessary for the calculation of the power loss area A_0 . This may be accomplished by applying the output voltage "e" of the search coil to the RC integrator circuit shown below in Fig. 3.1

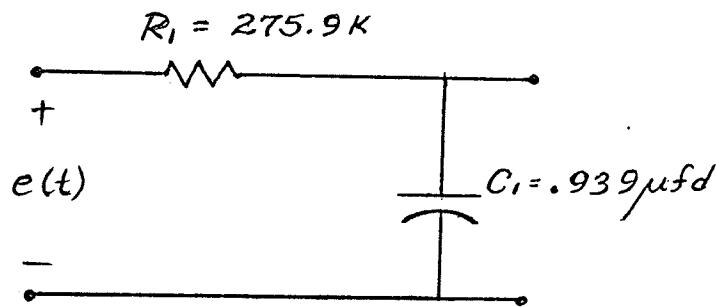


Fig. 3.1 INTEGRATION CIRCUIT USED TO OBTAIN $\int e dt$

The voltage transfer function of the above circuit is given as

$$\frac{E_2(s)}{E_1(s)} = \frac{1}{1 + R_1 C_1 s} \quad (3.1)$$

Values of $R_1 = 275.9K$ and $C_1 = .939 \mu fd$ were chosen so that the operating frequency $\omega = 377$ (60hz) radians/sec would be approximately two decades away from the "break" frequency $\omega_1 = 1/R_1 C_1 = 3.859$ radians/sec.

The result is that
$$\frac{E_2(s)}{E_1(s)} = \frac{1}{R_1 C_1 S} \quad (3.2)$$

3.2 Dimensions of Experimental Model

The basic transformer core was constructed in a square configuration with ten laminations per limb, each 36 x 6 x .012 inches. Each lamination consisted of high grade silicon steel, 12 mil Silectron W64 with a nominal loss of 1.41 watts/kilogram at 60 hz. (See Appendix - for detailed specification curves.) Clamping of the laminations to a 3/4" plywood base was provided by 3/4" wood blocks. Care was taken to try to use the same clamping pressure for all tests.

3.3 Establishment of Flux Density

Assuming the flux density to be sinusoidal in waveshape, a particular flux density required was obtained by energizing the core such that a desired value of voltage appeared at the output of the search coil. This voltage is obtained by the relationship derived in equation 2.4

$$E_{max} = \omega N_e A B_m \text{ volts}$$

A rectified-average sensitive digital voltmeter with a readout in an RMS scale was used. Therefore

$$E_{rms} = 266.4 N_e A B_m \text{ volts} \quad (3.3)$$

3.4 Power Loss Measurement

Examination of equation 2.13 reveals that the calculation of the power loss essentially involves the calculation of the area A_0 . Visual display

of the hysteresis curve may be obtained by applying the integrator circuit output voltage to the vertical amplifier and a voltage V proportional to i to the horizontal amplifier of the oscilloscope. The area A_o becomes

$$A_o = V_H \cdot V_V \cdot R_1 C_1 \cdot A_x \cdot \frac{1}{R_s} \quad (3.4)$$

where A_x = area of the oscilloscope display in cm^2

$R_1 C_1$ = integrator time constant

V_V = volts/cm of the vertical amplifier

V_H = volts/cm of the horizontal amplifier

R_s = series resistor = $.1\Omega$ used to obtain a voltage proportional to i .

The area of the oscilloscope display A_x was determined by a "dot grid" method whereby the area of a photographic enlargement of a polaroid photograph of the oscilloscope display of A_x was overlain with a fine grid of size $1\text{mm} \times 1\text{mm}$ and then the area obtained by counting the number of squares inside the enclosed area trace. The accuracy of this method was in the order of $\pm 1/2\%$. A sample grid and area trace is shown on the next page in Fig. 3.2 and 3.3.

Equation 2.13 may then be simplified to

$$P_o = 621.8 V_V V_H A_x \quad (3.5)$$

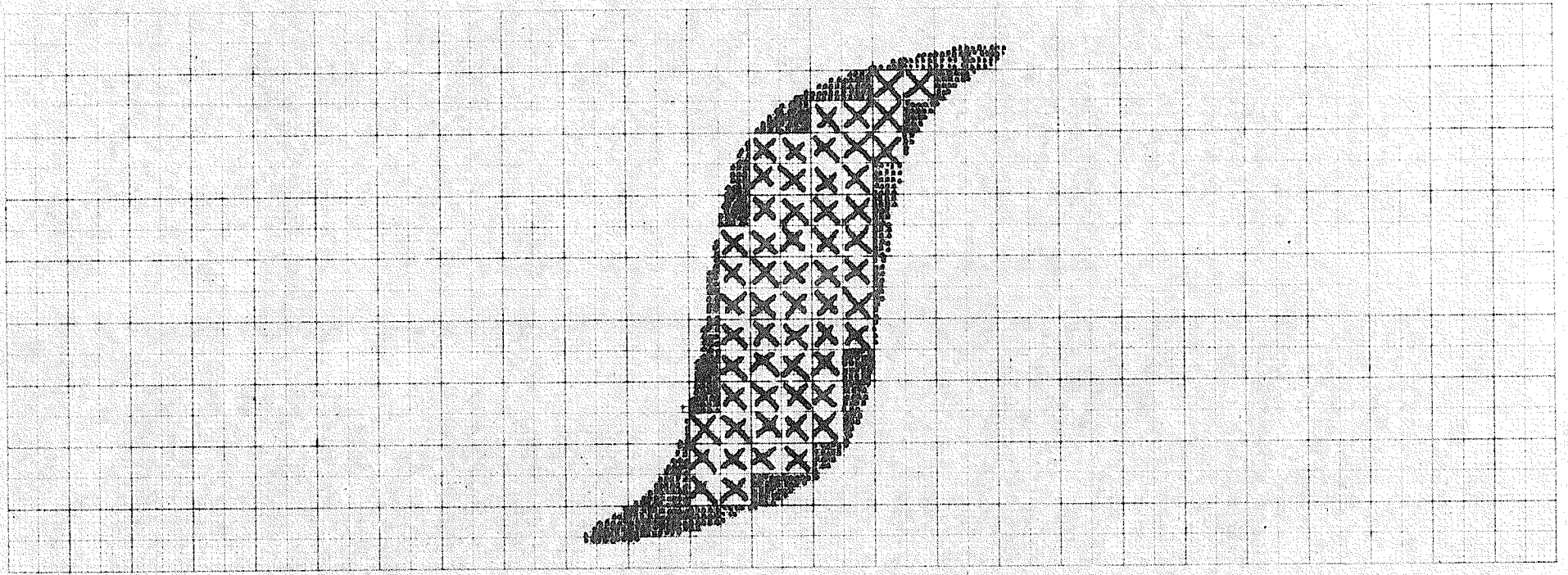


Fig. 3.2 Hysteresis Trace on Sample Grid

Chapter IV

EXPERIMENTAL INVESTIGATIONS

4.1 Core Construction Methods

In constructing the model core, three construction variables (refer to Fig's 4.1 and 4.2) are considered

- a) , air gap g in mm.
- b) overlap distance L in cm.
- c) method of stacking the laminations:
 - (i) alternate lapping with one lamination interval
 - (ii) alternate lapping with two lamination intervals
 - (iii) step-lapping

A flux density of 1.36 Tesla was established in each core configuration. Two values of air gap g , were used: 0 mm and 2 mm. Four values of overlap L were used: 0 , $.5$, 1 , and 2 cm. The overlap L shown in Fig. 4.1 was set accurately with a vernier gauge. The table shown on the next page illustrates the manner in which the various construction variables were considered.

Fig. 4.2 illustrates the overlap length L and the air gap g used in the various stacking methods. Fig. 4.3 illustrates the "alternate lapping" method of stacking the laminations and Fig. 4.4 illustrates the "step-lap" method suggested by Ellis and Burkhardt.⁽⁴⁾ Their suggestion of a step-lap greater than six times the lamination was used as a guide in setting a step-lap of 2 mm.

4:2 Apparatus and Test Set Up

The complete experimental set up along with all apparatus mentioned previously is shown in Fig. 4.5. The windings are mounted on hollow cylindrical fiberglass rods in such a manner that the laminations may be set into position, adjusted by vernier gauge, then removed with ease.

* See footnote on page 13

TABLE OF CONSTRUCTION VARIABLES

Lamination Lapping Interval	Flux Density T	Air Gap - g (MM)	Overlap Distance L (CM)	Area Display A_x
1	1.36	0	0	A_0
1	"	0	.5	A_1
1	"	0	1	A_2
1	"	0	2	A_3
1	"	2	2	A_4
2	1.36	0	.5	A_5
2	"	0	1	A_6
2	"	0	2	A_7
2	"	2	2	A_8
Step lap 2mm	1.36			A_9

*(From p. 12) It was originally intended that 1.5 Tesla be established as a core flux density. However, due to an oversight, eleven turns (instead of ten) were wound on each transformer core leg. This resulted in an actual flux density of $(10/11) \times 1.50$ or 1.36 Tesla.

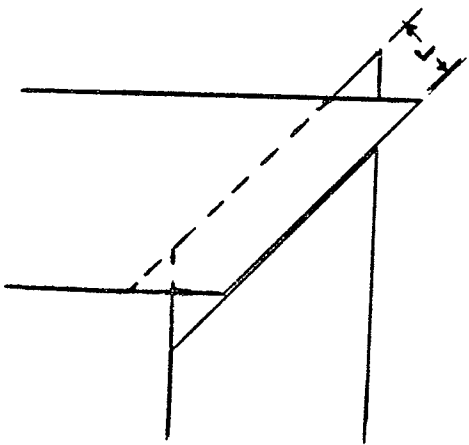


Fig: 4.1 45° mitered overlap joint of overlap length L

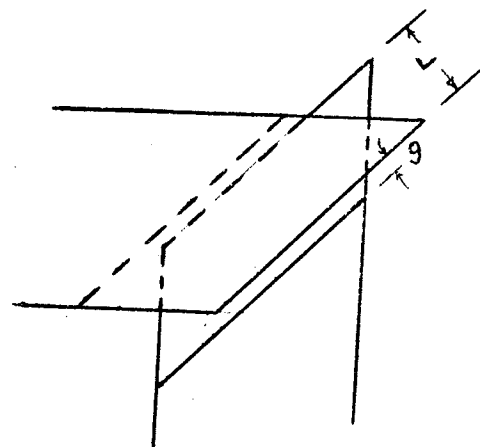
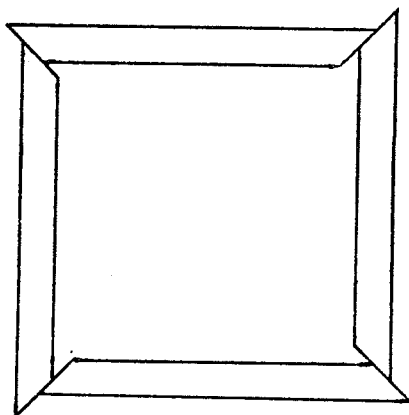
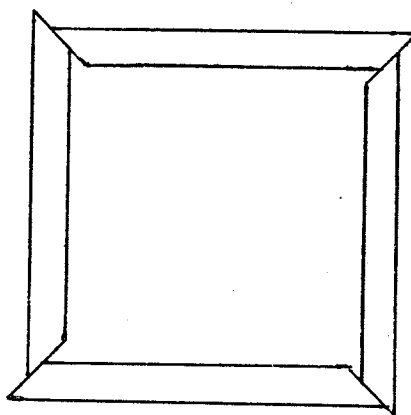


Fig: 4.2 45° mitered overlap P joint of overlap L and airgap g



odd layers



even layers

Fig. 4.3 Alternate Lapping Core Configuration

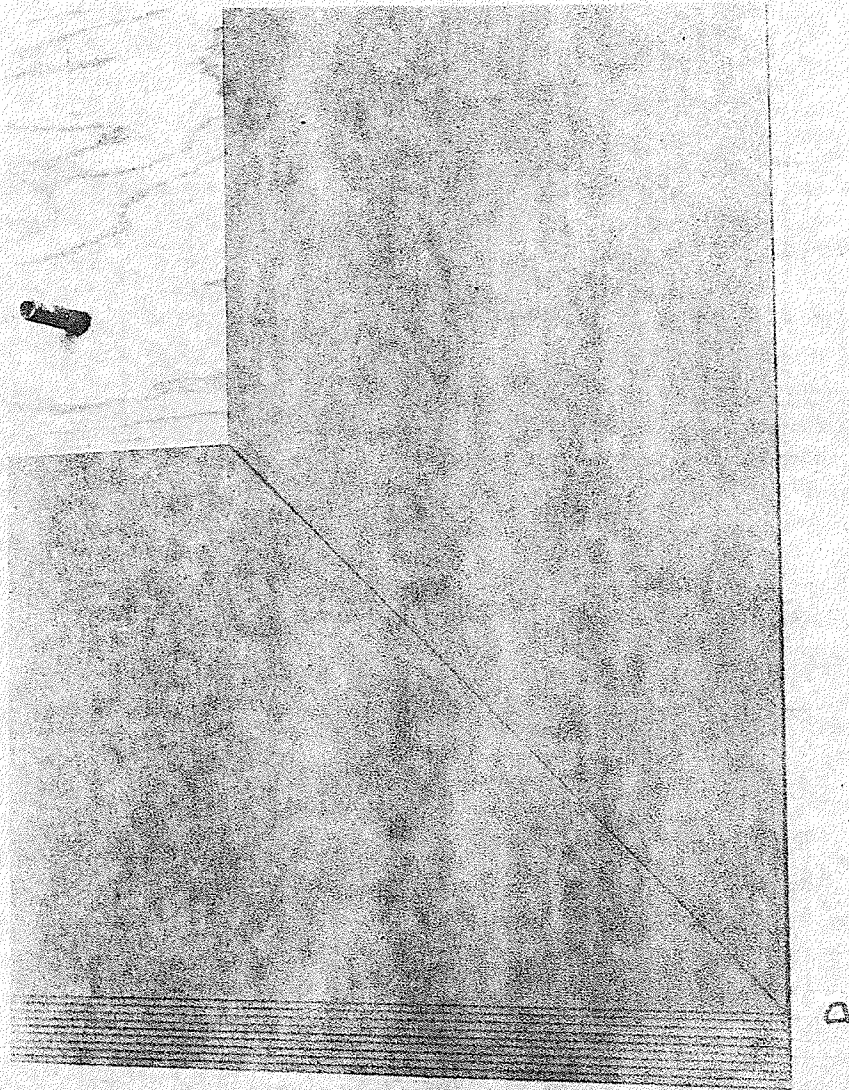


Fig: 4:4 Step Lap Method of laminating cores:

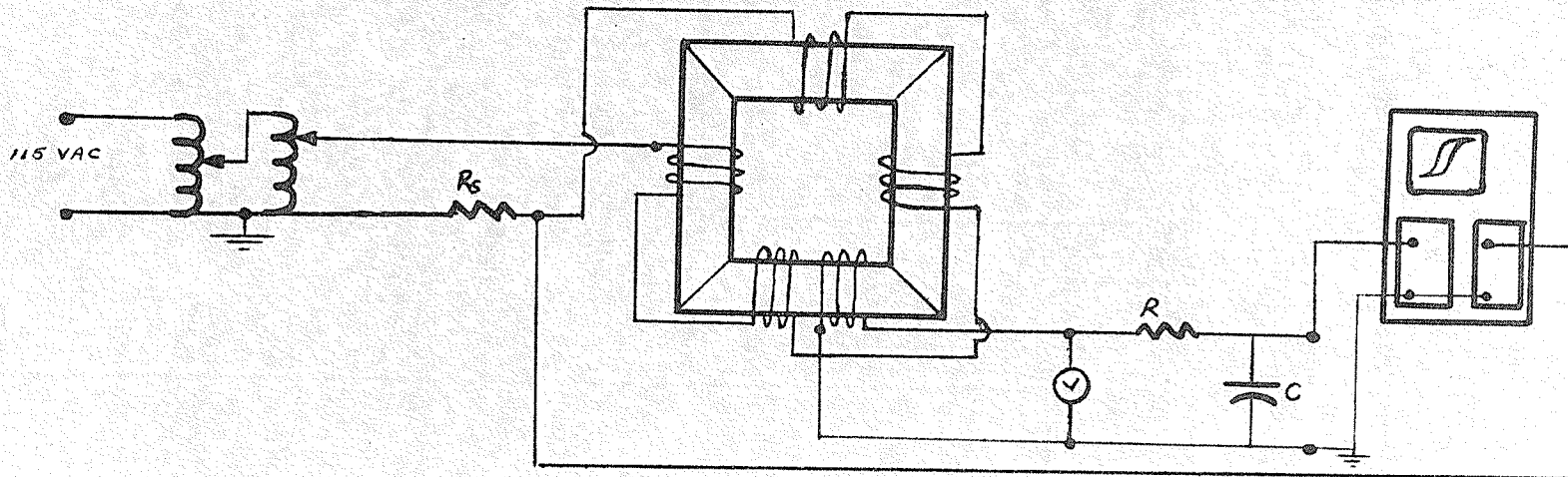
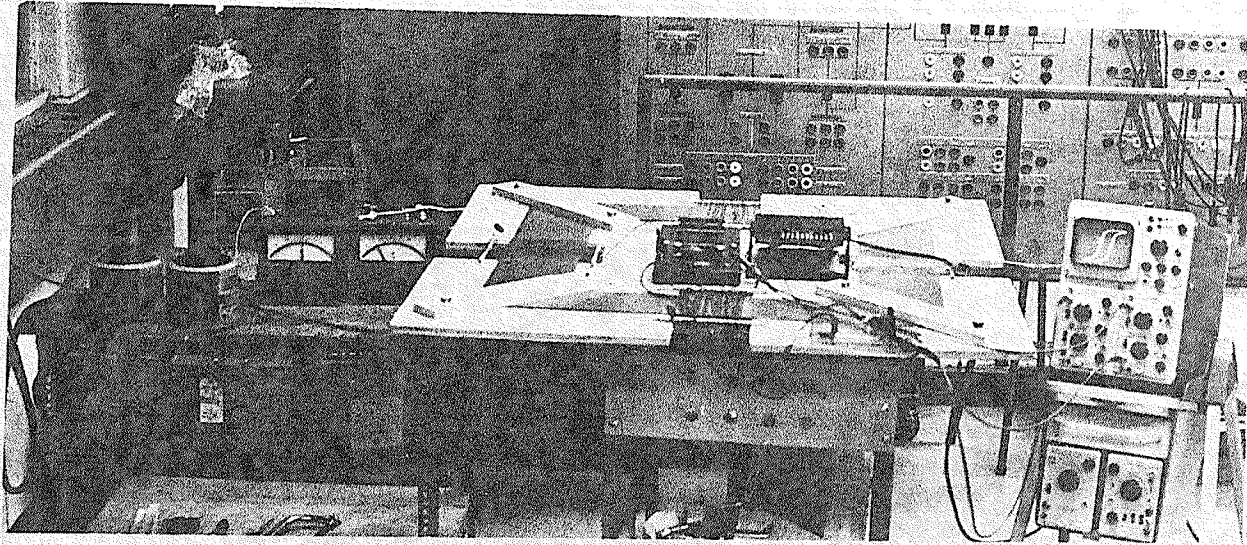


Fig. 4.5 Photograph and Schematic of Experimental Set-Up

(Refer to Fig. 4.6).

The input winding on each transformer core leg consisted of 11 turns of insulated number fourteen copper wire. The four windings (total of forty-four turns) were wound in the same direction to maintain the same direction of core flux. The construction of the search coil (adjacent to one of the series windings) was similar to that of the input windings; i.e. eleven turns of number fourteen wire. A nominal flux density of 1.36T and a volts per turn ratio of .225 provided an open circuit voltage of 2.25 V (maximum). This voltage was then measured by the digital voltmeter (refer Fig 4.7) then applied to the vertical amplifier of the oscilloscope. A resistor $R_s = .1\Omega$ was placed in series with the energizing winding to provide a voltage of sufficient amplitude which was then applied to the horizontal amplifier of the oscilloscope.

An RMS ammeter and voltmeter were used to measure the input RMS voltages and currents supplied from a variable voltage source consisting of two (2) fifteen amp (15 A) variacs connected in series. Care was taken to ensure high accuracy in the measurement of C_1 of the integrator circuit a Schering Bridge of five digit accuracy.

4.3 Power Loss Measurement

The area of the hysteresis curve displayed on the oscilloscope is essentially the hysteresis loss per cycle. The variacs were adjusted; thus energizing the core at a particular flux density. The average overall flux density of the core was found to be sinusoidal, so it was calculated by measuring the output voltage of the search coil. The flux density B_m has been given by the equation 3.2.

Upon obtaining the proper voltage for the desired flux density, the oscilloscope was adjusted for maximum display of the hysteresis curve. A

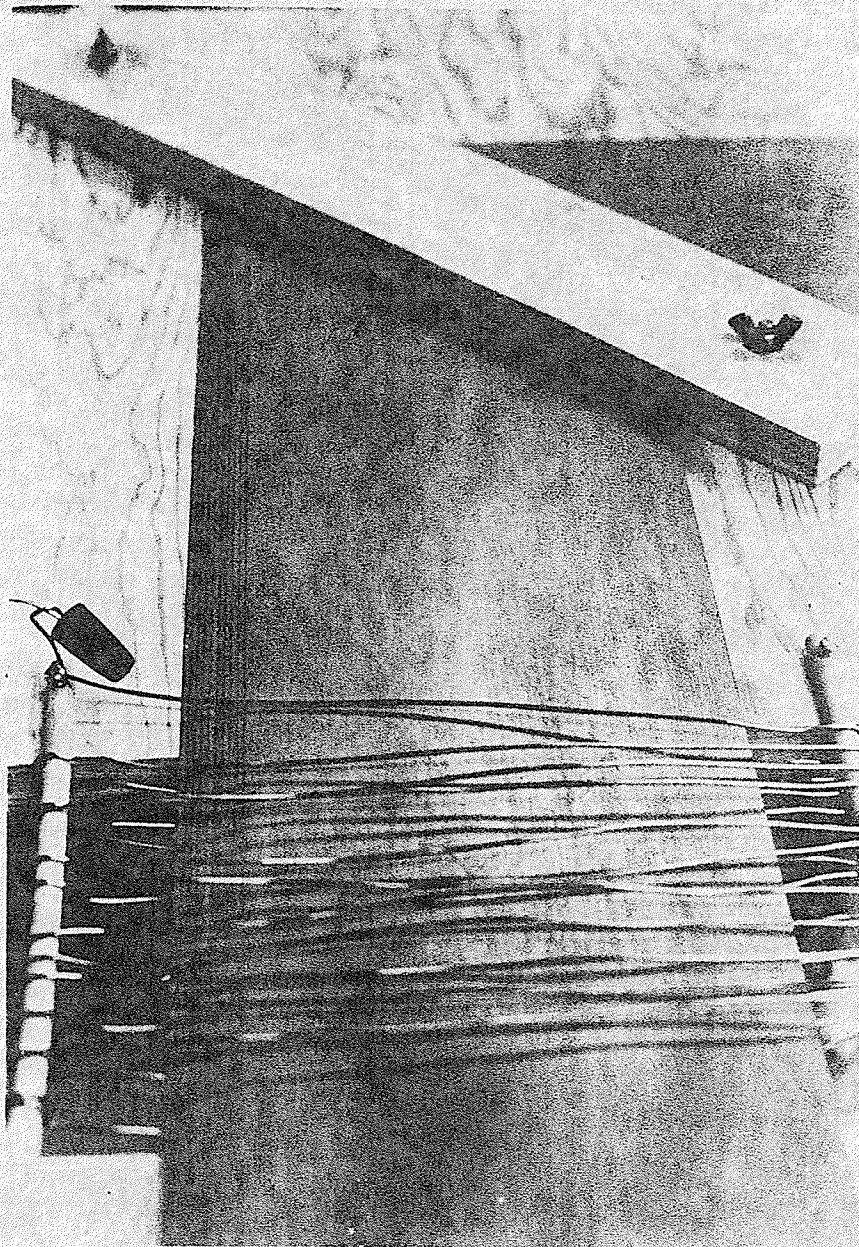


Fig. 4.6 Photograph of Excitation Winding on Transformer Core

photograph of the display was taken and then enlarged two hundred percent. The area of this photograph was then calculated by the "dot-grid" method and the result applied in equation 3.4.

Photographs were taken after repeated assembling and dismantling of the same core with different methods of lamination stacking, different overlap lengths at a flux density of 1.36 Tesla.

A sample oscilloscope display of the hysteresis curve displaying $\int \text{ed}t$ vs i is shown in Fig 4.8

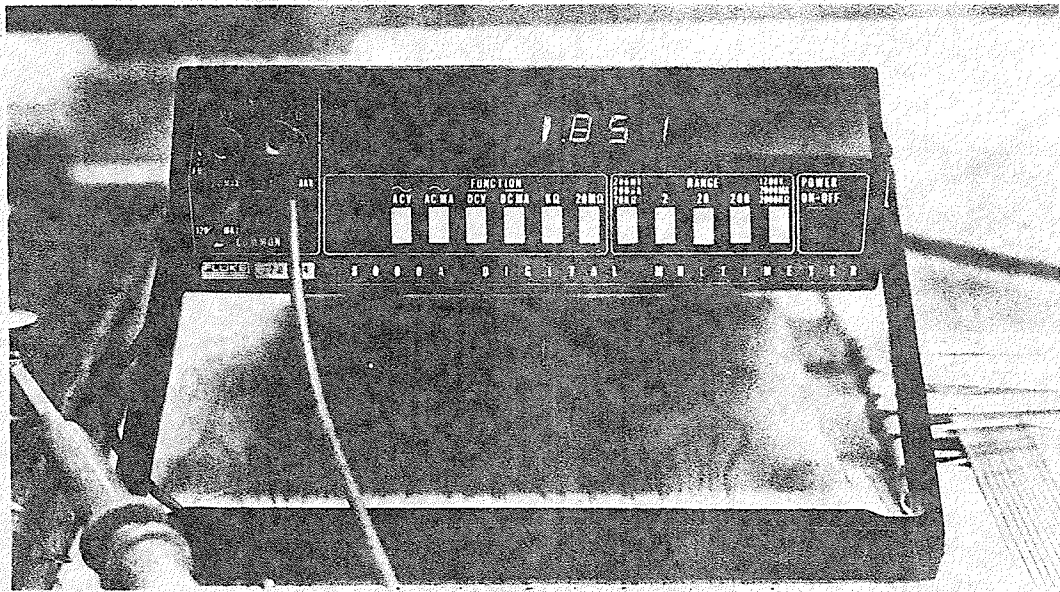


Fig. 4.7 Rectified Average Digital Read Out Voltmeter

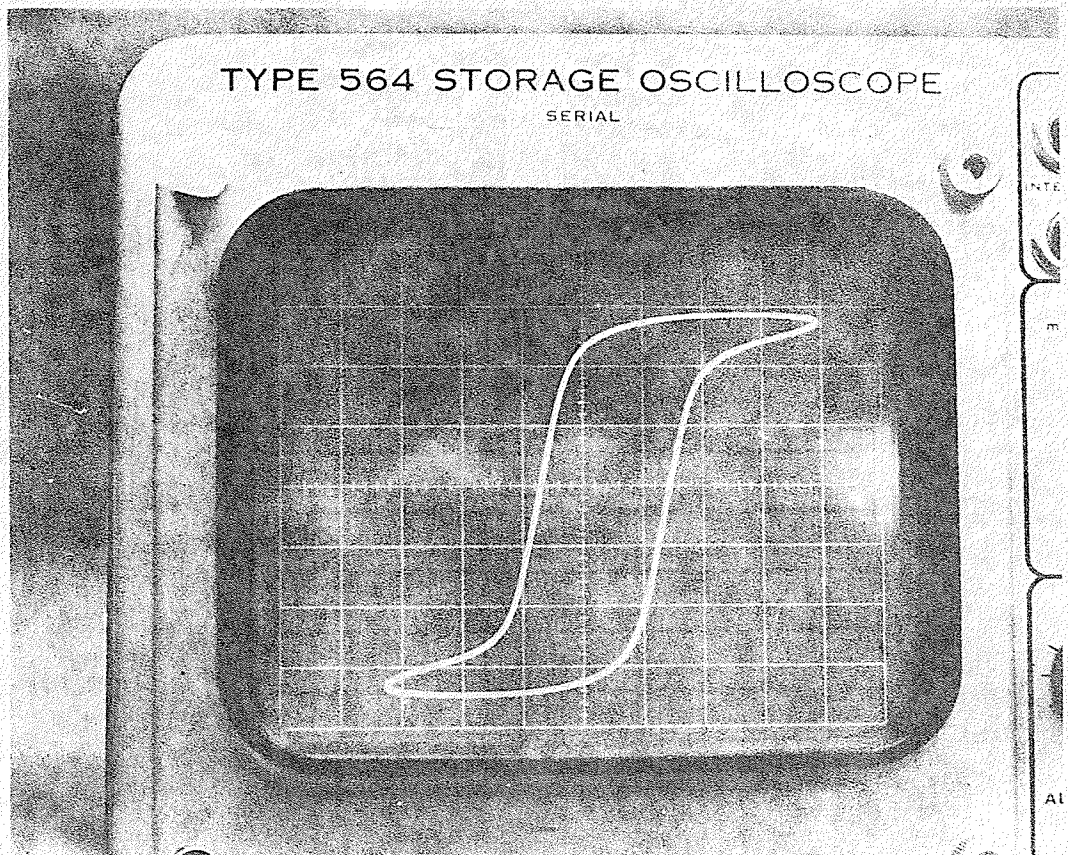


Fig. 4.8 Sample Oscilloscope Display of Hysteresis Curve

CHAPTER V

EXPERIMENTAL RESULTS AND ANALYSIS

5.1 GENERAL

Various core configurations were constructed as listed in Table 4.1. The experimental procedure has been explained in the previous chapter, and the results of the area and power loss calculations are listed in Table 5.1 shown on the following page.

The base loss of Table 5.1 is the minimum core loss measured, i.e. 10.646 watts. This minimum value occurred at an overlap L of .5cm and an airgap g of 0 mm. All other core loss values are referred to this minimum value.

A direct comparison of the results of Jones and that of the author cannot be made due to differences in certain variables of the measurement techniques. These differences are listed in Table 5.2. The most important differences are the flux density and the excitation frequency. However, on a per unit basis, the results show reasonable agreement at $L = .5\text{cm}$ and $g = 0\text{cm}$. The results of Jones listed in Table 5.1 are normalized to the minimum power loss (1.083 pu).

TABLE 5.1 EXPERIMENTAL DATA AT 1.36 TESLA

AREA* (cm ²)	OVERLAP L (cm)	AIRGAP g (mm)	POWER LOSS (P.L.) (watt)	PER UNIT POWER LOSS	PER UNIT POWER LOSS (JONES)	P _j ** (watts/in ² /joint)
A ₀ = 10.720	0	0	13.331	1.2522	1.135	.93220
A ₁ = 8.561	.5	0	10.646	1.0000	1.000	.0000
A ₂ = 8.746	1.0	0	10.876	1.0216	1.011	.07986
A ₃ = 9.299	2.0	0	11.564	1.0862	1.089	.31875
A ₄ = 11.000	2.0	2	13.679	---	---	---
A ₅ = 9.592	.5	0	11.928	1.1204	---	.44510
A ₆ = 9.374	1.0	0	11.657	1.0949	---	.35100
A ₇ = 9.586	2.0	0	11.921	1.1197	---	.44270
A ₈ = 11.033	2.0	2	13.720	---	---	---
A ₉ = 8.612	2 mm Step Tap		10.709	---	---	---

* Areas A₀, A₁, A₂, A₃, A₄, - single lamination interval

** P_j = excess loss above the minimum

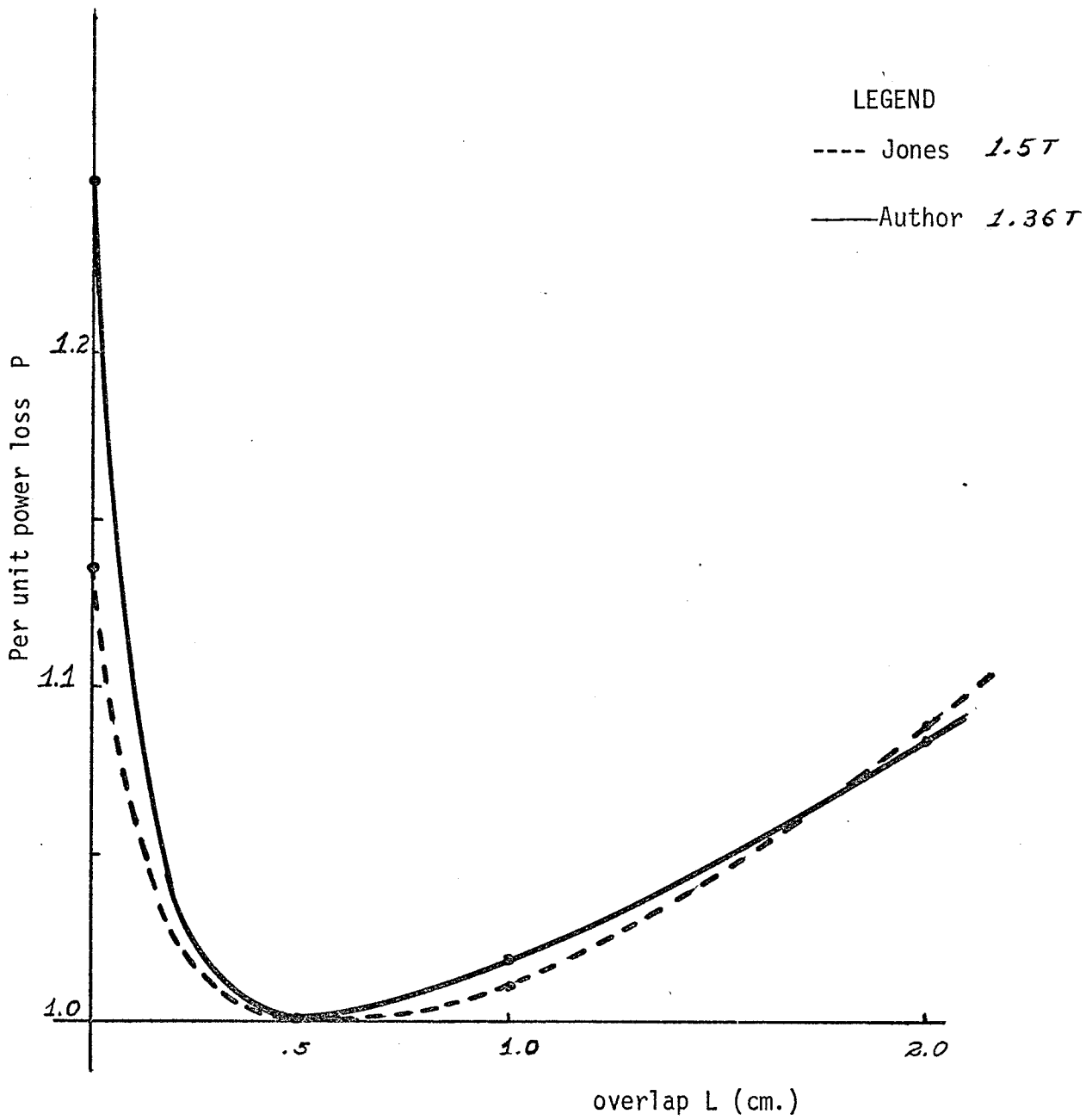


Fig. 5.1 Comparison of Measuring Techniques

TABLE 5.2 COMPARISON OF EXPERIMENTAL VARIABLES

<u>VARIABLE</u>	<u>JONES' TECHNIQUE</u>	<u>AUTHOR'S TECHNIQUE</u>
Lamination thickness	.013 in.	.012 in.
Lamination width	5.9 in.	6.00 in.
Lamination length	36.2 in.	36.00 in.
Standard overlap	.79 in.	.707 in.
Excitation frequency	50 hz	60 hz
Flux Density	1.5 T	1.36 T

The type of steel used in the model cores is probably somewhat different.

Fig. 5.1 illustrates the fact that an overlap length L does exist for which a minimum power loss occurs. If, in construction of a transformer core, a larger overlap $L = 1$ cm or 2 cm is selected (for added strength); an increase in core loss of 1 to 2% and 8.5% respectively will result, based on this particular configuration. A better basis for comparison is explained in the following section.

5.2 SINGLE LAMINATION INTERVAL RESULTS

The results (power loss values) for alternate lapping with single (one) lamination intervals have been presented in Table 5.1.

It has been stated previously that the total core loss consists of the eddy current and hysteresis losses. For a particular design of a transformer core joint, namely that of the 45° mitered joint, it was assumed (with reasonable accuracy) that the resulting core loss could also be attributed to two main components;

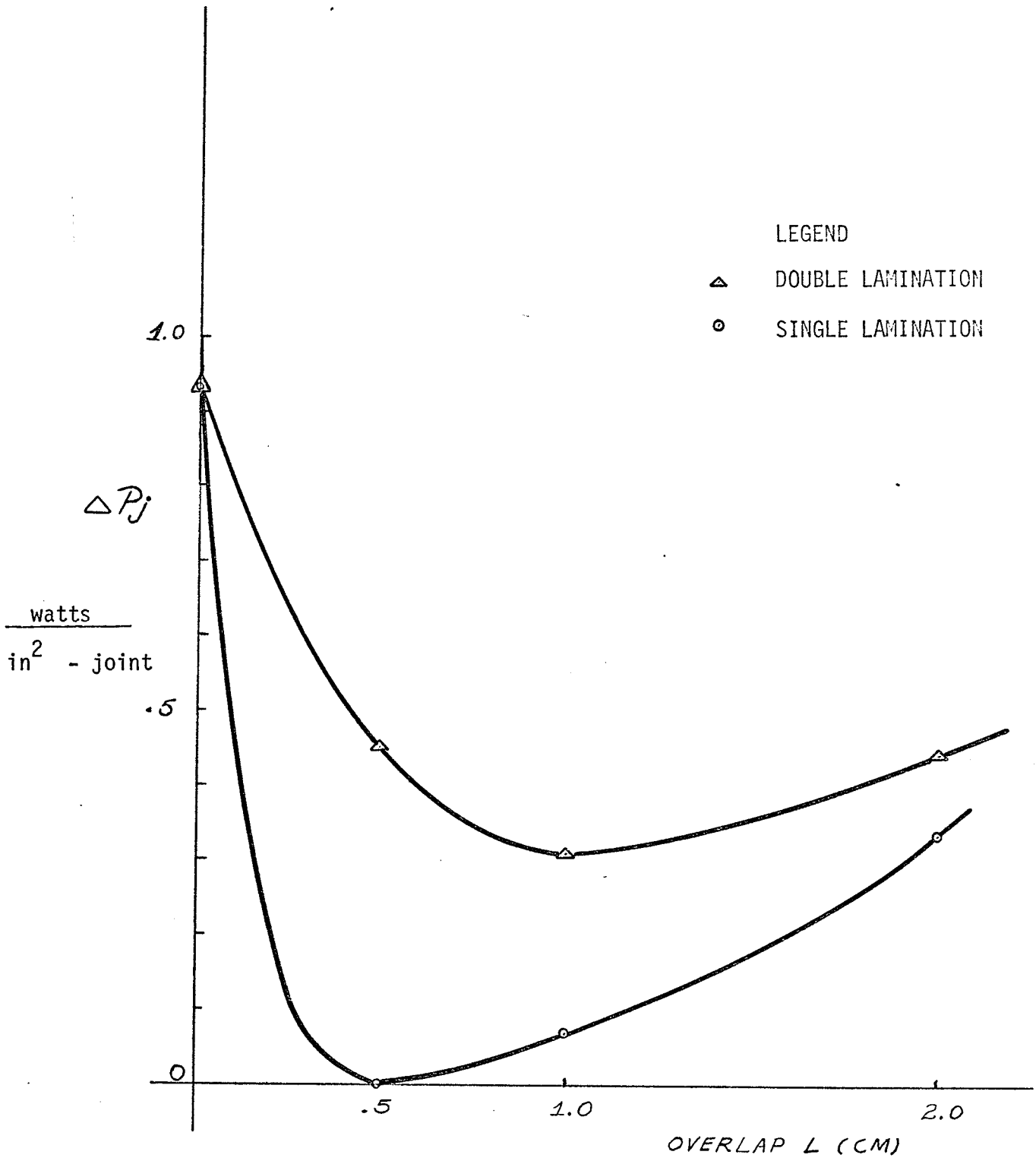


Fig. 5.2 Experimental Results of Alternate Lapping

- a) the power loss P_e associated with the iron losses of the transformer leg. These losses were assumed constant and proportional to the weight of the steel.
- b) the power loss P_j associated with the losses (in the 45° mitered joint) proportional to the area of the corner joint* and the number of corner joints.

Since the physical weight and number of laminations remained constant, it was assumed that the losses associated with the transformer steel were constant for all experimental configurations and that any change in the total core loss was therefore "in the joint itself", meaning increased loss in the immediate vicinity of the joint. Under this assumption, the single lamination results are represented again in Fig. 5.2 Here the vertical axis is ΔP_j , the increase in loss due to the joints alone, (normalized to the minimum loss $10.646W = 1.0$ p.u.) versus the overlap distance L (cm) at zero airgap (mm). The loss ΔP_j was assumed to be the core loss of four mitered corner joints whose area was taken as the cross-sectional area. Hence, the changes (increases) in power loss values were divided by the area ($.72 \text{ in}^2$) then divided again by four (4) in order that the result (ΔP_j) be expressed in watts/in^2 - joint.

Presentation of the results in the above mentioned manner has certain advantages. From the previous definition of ΔP_j , $\Delta P_j = 0$ at $L = .5\text{cm}$. If in the design of a transformer core, an overlap of 1 cm is chosen, Fig. 5.2 (or Table 5.1) illustrates the fact that the corner joint loss will increase by an amount $\Delta P_j = 7.98\%$ over the minimum value. By similar analysis an increase of 31.87% will result for a 2 cm overlap.

* and hence proportional to the leg cross-sectional area

5.3 DOUBLE LAMINATION INTERVAL RESULTS

The results for alternating lapping with a double lamination interval have been recorded in Table 5.1 and Fig. 5.2 simultaneously with those results for single lamination intervals. Examination of Fig. 5.2 reveals that the minimum power loss occurs at an overlap distance of 1 cm even though this minimum is 35.1% above single lamination minimum at .5cm. Also, the increase in power loss of values of .5 cm and 2 cm overlap over the minimum, are, for all practical purposes, identical. The 2 cm overlap value would be preferable in transformer construction and design since this overlap would provide more strength and rigidity to the core with a minimal increase in power loss.

5.4 AIRGAP CONSIDERATIONS

The measured core loss values for an airgap g of 0 mm and 2 mm at an overlap length of 2cm are listed in Table 5.3 below. The increase in core loss of the 2mm airgap configurations (as compared to the core loss for zero airgap) was found to be 18% for single lamination intervals and 15% for double lamination intervals.

TABLE 5.3 VARIATION OF CORE LOSS WITH AIRGAP AT AN OVERLAP DISTANCE $L = 2\text{cm}$

<u>LAMINATION INTERVAL</u>	<u>$g = 0\text{mm}$</u>	<u>$g = 2\text{mm}$</u>	<u>% increase</u>
single	11.564 watts	13.679 watts	18.2%
double	11.921 "	13.720 "	15 %

5.5 STEPLAP CONSIDERATIONS

The power loss measured in this configuration was 10.709 watts (see Table 5.1). This represents an increase in the order of 1/2% above the minimum power loss configuration at $L = .5\text{cm}$, $g = 0\text{mm}$. Although the power loss measured resulted in a slight increase over the minimum loss configuration, it should be made clear that this change in power loss could have been zero or perhaps even appeared as a decrease below the minimum case. Extremely accurate setting of the step-lap configuration was limited by the tolerances in the cutting of the core steel. It still remains to be seen whether or not there exists a step lap configuration for which the resulting power loss will be less than that of the minimum loss case ($L = .5\text{cm}$).

Although the magnitudes of power loss for the step-lap joint and single lamination butt-lap joint are almost identical, the step-lap configuration required a much lower magnitude of volt-ampere (VA) excitation for the same flux density. The magnitude of excitation for the step-lap configuration was found to be 15.444 VA as compared to 21.498VA for the butt-lap case. The improvement was in the order of 28%.

The VA excitation magnitudes of all experimental configurations are listed in Appendix A.

5.6 APPLICATION TO A PRACTICAL CASE

The experimental results of Fig. 5.2 may be applied to a typical single phase, 80 MVA power transformer whose specifications are listed below in Table 5.4

TABLE 5.4 POWER TRANSFORMER SPECIFICATIONS

Total Weight 80,000 lbs

Total Core Loss 60 KW

Measured Core Loss .75w/lb

Design Flux Density = $101 \text{ kI/in}^2 = 1.57 \text{ T}$

Overlap distance = 1.8 cm

Cross Sectional Area = 740 in^2

Examination of Fig. 5.2 at an overlap distance $L = 1.8 \text{ cm}$ reveals that $\Delta P_j = .42$ and $.27 \text{ watts/in}^2$ - joint respectively. The following observations are in order;

- a) If the transformer core is stacked in single lamination intervals instead of double lamination intervals, the loss in the joints would have been reduced by

$$(.42 - .27) \frac{\text{watts}}{\text{in}^2 - \text{joint}} \times 4 \text{ joints} \times 740 \text{ in}^2 = 440 \text{ watts}$$

which is .7% of the measured core loss.

- b) If the transformer core is stacked in single lamination intervals and the overlap reduced to .5cm, the loss would have been reduced by

$$.42 \frac{\text{watts}}{\text{in}^2 - \text{joint}} \times 4 \text{ joints} \times 740 \text{ in}^2 = 1.24 \text{ KW}$$

which is 2.1% of the measured core loss.

- c) With step-lap joints, the reduction would again be about 2% as in part(b). The exciting current may be reduced by approximately 40% for a step lap joint as compared to 2 cm overlap, zero air-gap core configuration.

CHAPTER VI

CONCLUSIONS

The proposed method of measuring/calculating the total core loss in an experimental core has proven to be one of good accuracy; the results comparing favourably to a published work in the same field of research. The results were presented in a manner with which one may predict with ease the power loss increase over and above the minimum loss configuration. An optimum overlap length exists for each of the methods (of stacking laminations) investigated. The experimental core constructed with single laminations had an optimum overlap at .5cm while the experimental core with double or paired laminations had an optimum overlap at 1 cm. The double lamination configurations appeared to have higher losses for all values of overlap as compared to the single lamination configuration.

Increasing the airgap increases the core losses. Core configurations with airgaps increased from 0 to 2 mm were found to have core loss increases of 10% and 15% for single and double lamination intervals respectively.

The improvements in performance with the step-lap core over those made with butt lap joints proved to be equally satisfactory if not superior. A manufacturer can obtain a given performance level with a smaller unit, which implies savings in labor and raw materials. The user is rewarded with a more efficient piece of equipment having a lower cost of operation. It appears that a comprehensive study to determine the relationship between power loss and various step-lap sizes would be very valuable.

BIBLIOGRAPHY

- [1] M. A. Jones, A. J. Moses, and J.E. Thompson,
"Flux Distribution and Power Loss in the Mitered Overlap
Joint in Power Transformer Cones," IEEE Transactions on Magnetics,
June 1973, MAG-9, No. 2, pp 114-122
- [2] G. R. Slemon, "Magneto Electric Devices,
John Wiley and Sons, Inc., New York 1966
- [3] "Electrical Materials Handbook," Allegheny Ludlum Steel Corporation,
Pittsburgh, PA., Ch. 9.
- [4] B. B. Ellis and C. E. Burkhardt, "Performance and Production of Step-
Lap Joints in Stacked Cores," Insulation/Circuits, Nov. 1973

APPENDIX A

The experimental data accumulated is shown in the table below. For all core configurations with a flux density of 1.36T the values of V_V and V_H necessary for application in equation 3.5 were found to be .01V/cm and .2V/cm respectively.

VOLT-AMPERE INPUT DATA

OVERLAP L(cm)	AIRGAP g(mm)	V_{RMS}	I_{RMS}	VA [*]
0	0	7.60	4.42	35.592
.5	0	8.70	2.47	21.489
1.0	0	8.80	2.70	23.760
2.0	0	8.84	2.75	23.410
2.0	2	9.38	4.71	44.180
.5	0	8.75	2.73	23.887
1.0	0	8.80	2.88	25.344
2.0	0	8.81	2.90	25.549
2.0	2	9.35	4.84	45.254
Step lap of 2 mm		8.58	1.80	15.444

* These values include the losses of the .1 ohm shunt.

APPENDIX B

MANUFACTURER'S PUBLISHED CURVES

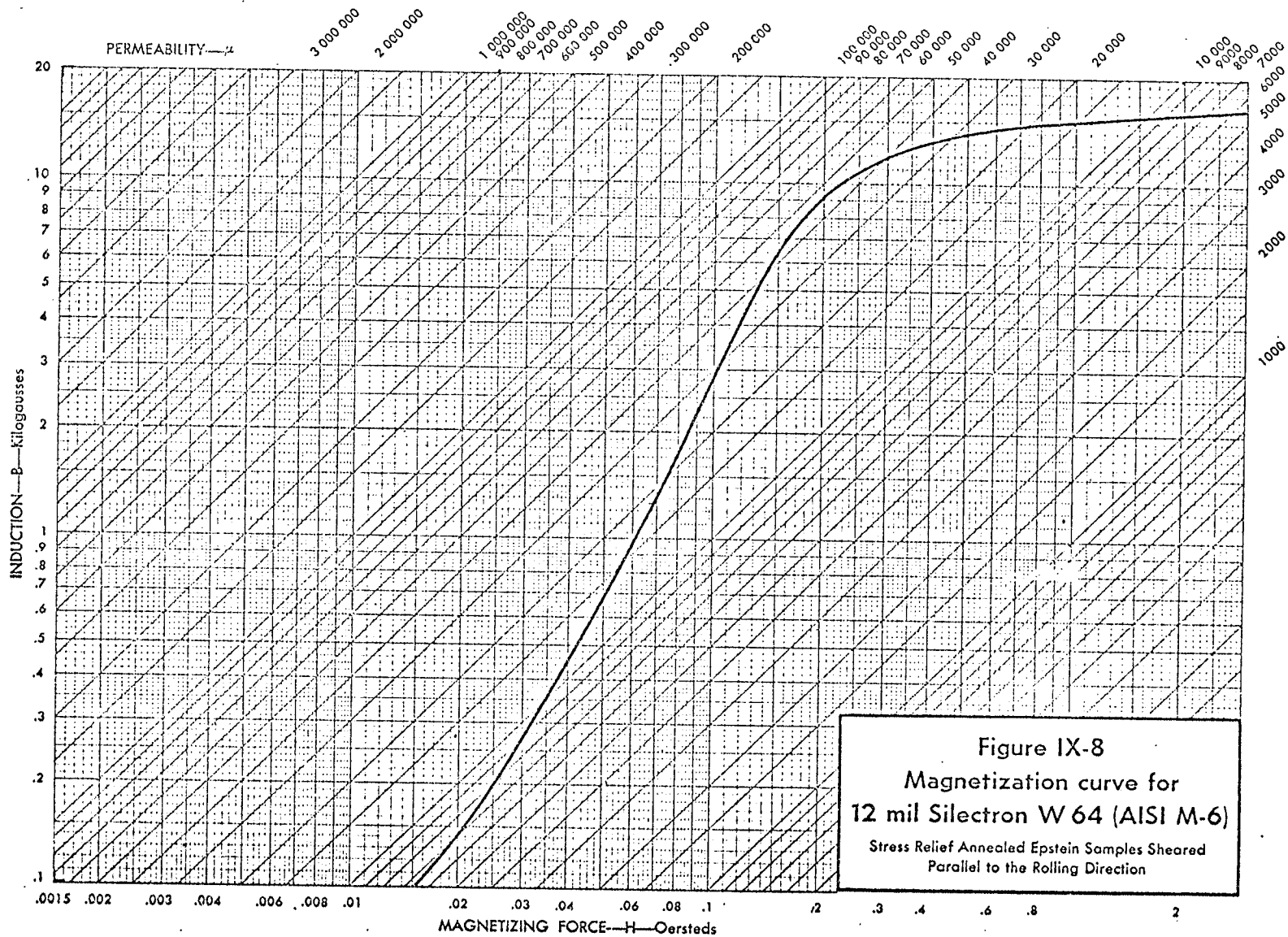


Figure IX-8
Magnetization curve for
12 mil Silectron W 64 (AISI M-6)
Stress Relief Annealed Epstein Samples Sheared
Parallel to the Rolling Direction

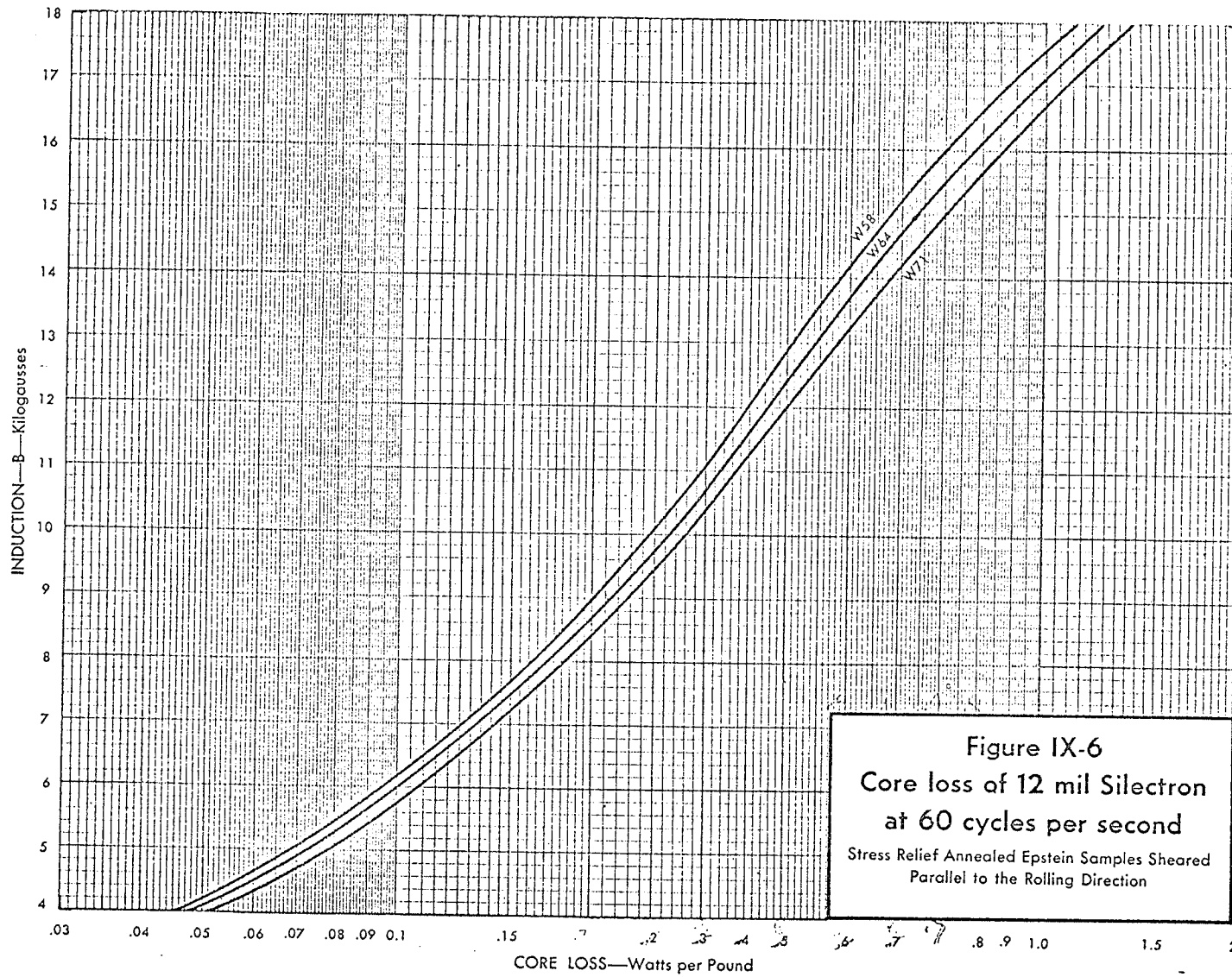
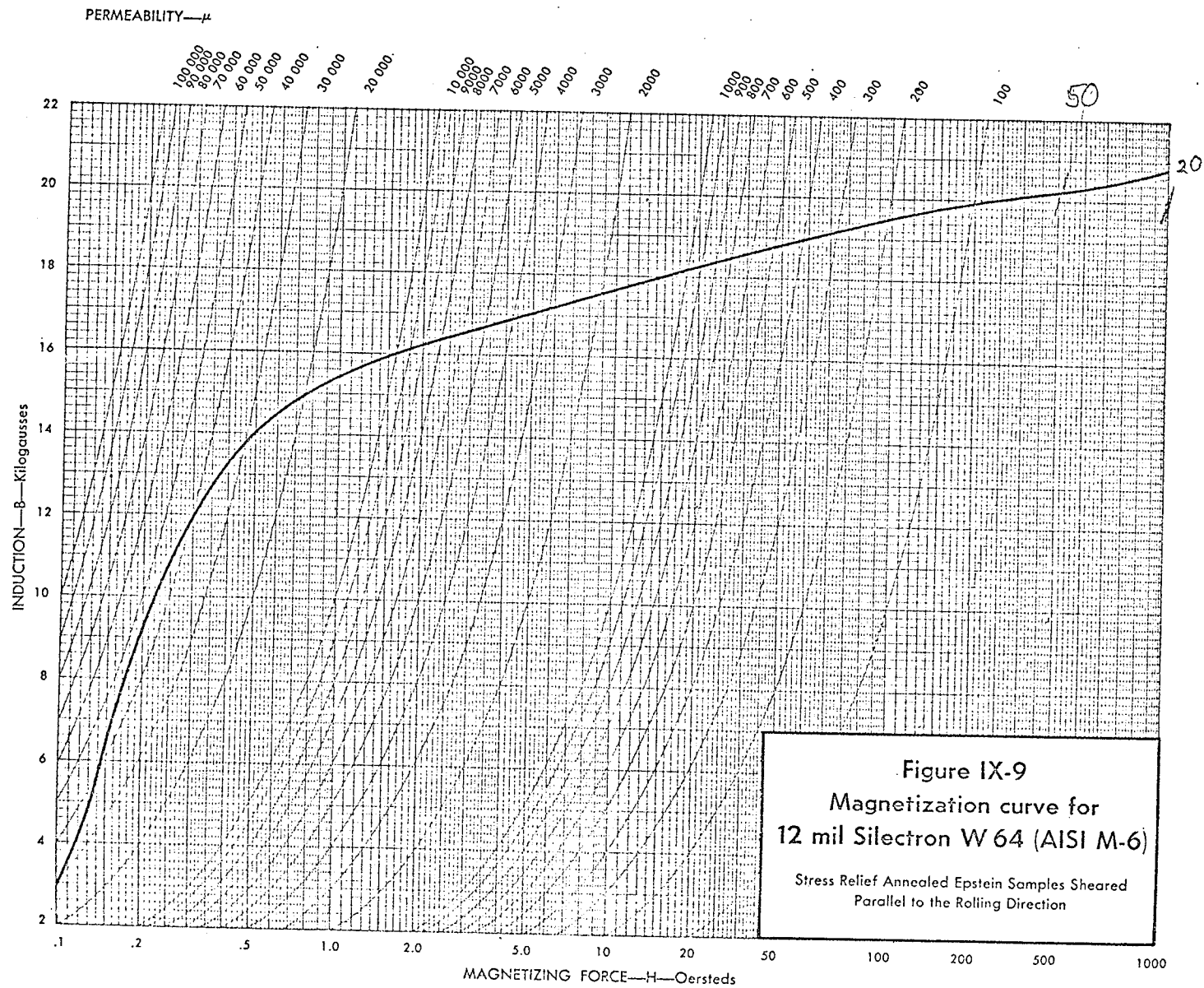


Figure IX-6
 Core loss of 12 mil Silectron
 at 60 cycles per second
 Stress Relief Annealed Epstein Samples Sheared
 Parallel to the Rolling Direction



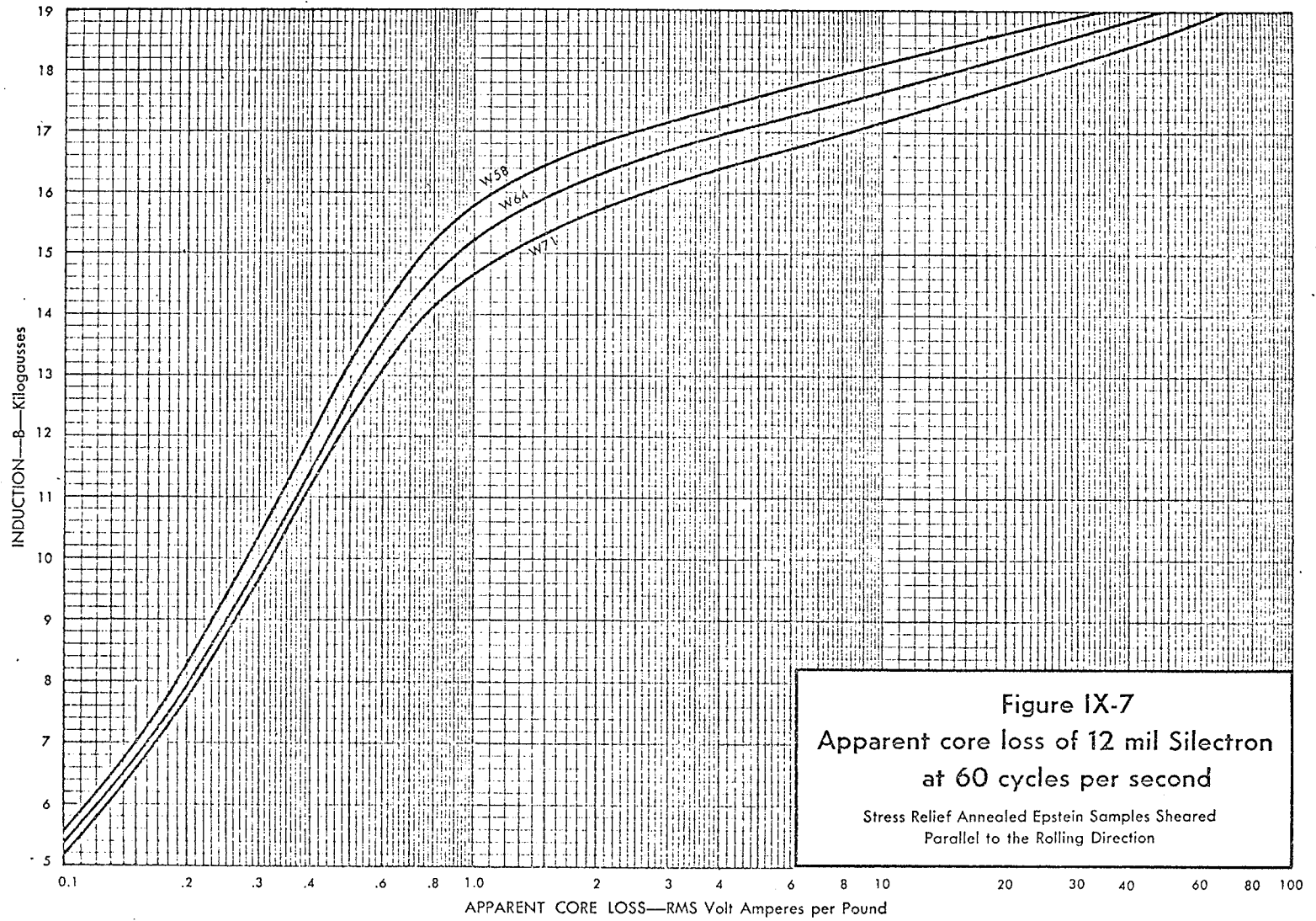


Figure IX-7
 Apparent core loss of 12 mil Silectron
 at 60 cycles per second
 Stress Relief Annealed Epstein Samples Sheared
 Parallel to the Rolling Direction